

## The effect of metal objects on the SAR and temperature increase in the human head exposed to dipole antenna (numerical analysis)

Deepshikha Bhargava <sup>a</sup>, Phadungsak Rattanadecho <sup>a,\*</sup>, Teerapot Wessapan <sup>b</sup>

<sup>a</sup> Center of Excellence in Electromagnetic Energy Utilization in Engineering (CEE), Department of Mechanical Engineering, Faculty of Engineering, Thammasat University (Rangsit Campus), 99 Moo 18, Klong Luang, Pathum Thani, 12120, Thailand

<sup>b</sup> Department of Mechanical Engineering, Faculty of Engineering, Rajamangala University of Technology Thanyaburi, 39 Moo 1, Rangsit-Nakhonnayok Rd. (Klong6), Pathum Thani, 12110, Thailand



### ARTICLE INFO

#### Keywords:

Electromagnetic waves  
SAR  
Temperature  
Dipole antenna  
Metal object

### ABSTRACT

Wearable metal objects with high electromagnetic reflection characteristics can cause interference with the incident waves during exposure to the electromagnetic (EM) radiation. Therefore, it is of interest to investigate the effect of metal objects capable of increasing the absorption of EM energy and temperature within the tissues when get exposed to EM radiation. A numerical analysis of increase in specific absorption rate (SAR) and temperature distribution in a human head model when metal objects are placed between the head and radiating source is performed. A realistic three-dimensional heterogeneous human head model, metal objects of different shapes and sizes, and spectacles with different lenses are used. A half-wavelength dipole antenna operating at 1800 MHz served as an EM radiation source. Results show that the presence of metal objects in proximity to the head alters SAR and temperature increase within the tissues. In most cases, metal objects redistribute the EM field incident upon them to a smaller region increasing power absorption, thereby increasing SAR and temperature in that region. The power absorption in head layers is found to be sensitive to metal object's size and shape, and distance of the antenna from the objects.

### 1. Introduction

The concern that EM waves are affecting human tissues adversely has been widely discussed over a decade. The matrix which is used to show the amount of absorption of electromagnetic (EM) radiation in the tissue is known as Specific absorption rate (SAR) [1]. SAR can be determined by dividing the power dissipation normalized in the tissue to the density of the tissue. Organizations, such as ICNIRP and IEEE have released guidelines based on the SAR values to limit the exposure of EM waves [2–4]. However, the absorption of EM radiation in the tissues increases the temperature within it which is known to be the main cause of biological hazards [5,6]. There have been researches discussing the importance of studying SAR as well as temperature increase inside the tissues exposed to EM radiations [7–9]. Hirata et al. [10], in their numerical analysis, irradiate the human eye using plane wave of 600 MHz to 6 GHz and showed that SAR and temperature can have different hot spot regions inside the tissues which depend on the size of the tissues and the radiating frequency used. Bernadi et al. [11], exposed human head model to different types of mobile phone antennas and found that SAR and temperature do not correspond to each other. Dielectric properties, thermal properties as well as the anatomy of the tissues

\* Corresponding author.

E-mail address: [ratphadu@engr.tu.ac.th](mailto:ratphadu@engr.tu.ac.th) (P. Rattanadecho).

## Nomenclature

<i>C</i>	specific heat capacity ( $J/(kg \cdot ^\circ C)$ )
<i>E</i>	electric field intensity ( $V/m$ )
<i>f</i>	frequency of incident wave (Hz)
<i>j</i>	current density ( $A/m^2$ )
<i>k</i>	thermal conductivity ( $W/(m \cdot ^\circ C)$ )
<i>n</i>	normal vector
<i>Q</i>	heat source ( $W/m^3$ )
<i>T</i>	temperature ( $^\circ C$ )
<i>t</i>	time

have their influence on them. Our research group has also been studying the distribution of electric field, SAR, and temperature in the different parts of the human body including the torso, head, liver, etc. caused by in getting contact with near and far-field EM radiating sources. It has been found that structure of the radiating source, and distance of the radiating source from the tissue plays an important part in the absorption of EM radiation [12–14].

Among all the EM radiation emitting sources humans get exposed to in daily life, mobile phones have been the most frequent source of near field exposure, and hence the reason for concern for our health. There has also been a concern that the metallic implants in the presence of EM radiation can alter the absorption of EM energy in the tissues [15–21]. McIntosh et al., studied the exposure of mobile phone radiation for cochlear implant users and discussed the resonance effect and constructive interference effect for titanium cranioplasty plate inside the head. They found no significant difference in the EM absorption in presence of the implant plate [16,17]. Olteanu et al. studied metallic carotid stent implant effect in a simple spherical head and did not find temperature to exceed above safety threshold  $1^\circ C$  [18]. Virtanen et al. investigated the effect of varying size, position and orientations of implants on the SAR in the tissues. They found that implant situated deeper in the tissue cause more absorption than situated on the surface of the skin [19,20]. Fernandez et al. studied the effect of the ear-piercing metals exposed to a near field EM radiating source and found an increased value of SAR [21]. Joo et al. [22], also found an increased value of SAR in a child and an adult head model wearing spectacles and implant behind the ear.

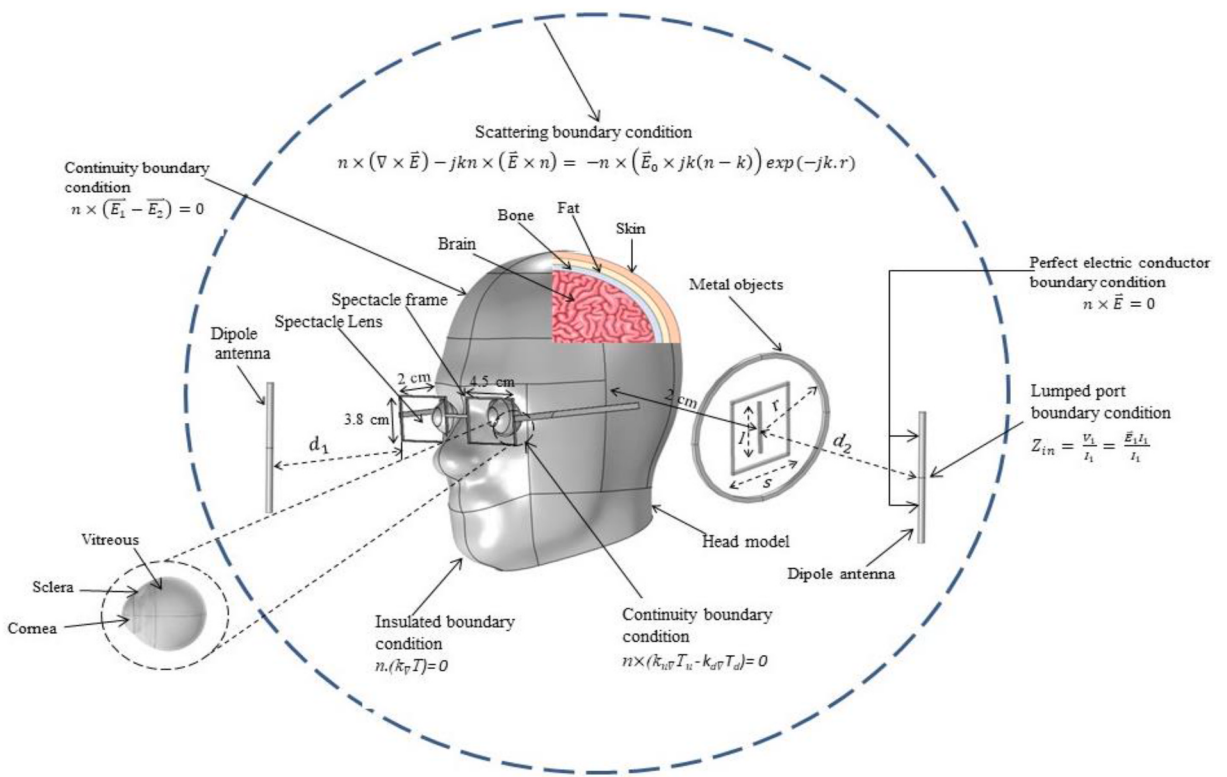


**Fig. 1.** Boundary conditions applied for the analysis of EM wave propagation and heat transfer on the heterogenous head model surrounded by different types of metal objects and a dipole antenna in the voice and video calling positions.

Not only metals situated inside the tissues, but the effect of metal objects outside of the tissues has also been studied. Whittow et al. [23–26], have extensively investigated the effects of metals mainly jewelry and spectacles, on the human tissues by both experimental and numerical methods. In their studies, they irradiate the head from in front like a personal data assistant device and calculate the SAR in the eyes for with and without spectacles. SAR obtained in the eyes for both cases showed that wearing spectacles can increase or decrease the SAR in the eyes, which depends more on the shape of the spectacles and the frequency used and less on the lens of the spectacles. They also investigated change in SAR when metal pins and rings were situated in the proximity of the head. The head was irradiated with microwave communication equipment at different frequencies. They found that pins and rings of resonant sizes can double the SAR in the head. Lan et al. [27], found that using eyewear devices such as Bluetooth with glasses can form new hotspot regions in the ocular tissues which increase the SAR in the eyes.

However, the investigation of temperature increases inside the tissues due to metal objects in its proximity is limited. The models considered for the study are either very simple or do not discuss in detail the power absorption in the different layers of the head. Hence, in this paper, a detailed study on the EM absorption inside the different layers of the human head when metal objects of different sizes and shapes are present is studied. A realistic heterogeneous model of the human head including 4 layers of skin, fat, bone, and brain and 3 layers of eyeball including sclera, cornea, and vitreous has been used from our previous studies [9,14,28]. A half-wave dipole antenna operating at 1800 MHz is used for the EM radiation source. The attention is paid on the increase in SAR and temperature in the head model layers by the metal objects (jewelry and spectacle) situated nearby the head. The metal objects are placed 2 cm away from the head and the dipole antenna is placed at various distances from the metal. Two cases, voice calling and video calling, are considered depending on the dipole position around the head. The coupled model of EM wave propagation and bioheat transfer are numerically solved by FEM (finite element method). Maxwell equations are used to determine the absorbed EM wave and Pennes' bioheat equation is used to study the temperature increase in different tissue layers.

## 2. Problem formulation

### 2.1. Head, metal object, and dipole antenna models

A 3D heterogeneous head consists of skin, fat, bone, brain, sclera, vitreous, and cornea. Metal objects used are of four types: a pin, a ring, a square and a spectacle, shown in Fig. 1. In the analysis, the size of the metal objects varies while thickness 2 mm stays constant. Metal objects of these shapes can be related to the jewelry worn near to the head area such as earrings, and hairpins. A spectacle of two types of lenses namely, PVC ( $\sigma = 4.46 \times 10^{-4} S/m$ ,  $\epsilon_r = 2.46$ ) and glass ( $\sigma = 0.0054 S/m$ ,  $\epsilon_r = 4.82$ ) has also been included in the study. The material used for all the metal objects is copper which is a PEC (perfect electric conductor) metal. Copper and other materials, such as gold and silver do not differ much in their conductivities and are equally used in making jewelry and spectacle frames [25]. For EM radiating source, half-wave dipole antenna operating at 1800 MHz frequency and 1 W radiating power has been used (Fig. 1). The frequency used for the analysis comes under the Global System for Mobile (GSM) Communications, hence can be related to the cases when a person talks on the phone or surfs the internet.

### 2.2. Elements of study

The objective of this study is to find out the effect of metal objects such as earrings, hairpins, spectacles worn in our daily life on the SAR and temperature increase in the head when exposed to near field radiation. For the analysis, metal objects of different shapes and sizes are placed at a distance of 2 cm from the head, as shown in Fig. 1. The dipole antenna radiating at 1800 MHz frequency is placed at various distances ( $d_1$  and  $d_2$ ) from the metals. Here, dipole antenna placed on the right side of the head model can be related to the voice calling position and when placed in front of the eyes can be related to the video calling position. Radius  $r$  of the ring, side  $s$  of the square, and length  $l$  of the pin, in voice calling position, are varied to find out the worst shape and size of the metals that affects the SAR and temperature most. Likewise, in video calling position, two types of lenses are used to see which lens affects the SAR and temperature most. Dielectric and thermal properties of tissues used in the numerical analysis are shown in Tables I and II, respectively, [6, 29]. COMSOL™ Multiphysics software based on FEM analysis [30], has been used for solving the coupled model of EM wave propagation and bioheat transfer. For reducing the computation time, the head model has been simplified. Head model without eyeball and spectacles is used when the head is irradiated from the ear side i.e. voice calling position. Spectacle with only one lens has been used out of the whole spectacle model when the head is irradiated from in front i.e. video calling position.

**Table 1**  
Dielectric properties of tissues at 1800 MHz [6,9].

Type of tissues	$\epsilon_r$	$\sigma (S/m)$
Skin	32.5	0.52
Fat	5.35	0.078
Bone	8.0	0.16
Brain	53.0	1.7
Sclera	52.70	1.68
Vitreous	73.70	2.33
Cornea	55.0	2.32

**Table 2**

Thermal properties of tissues [6,9].

Type of tissue	$\rho$ (kg/m <sup>3</sup> )	$k$ (W/m°C)	$C$ (J/kg°C)	$Q_{met}$ (W/m <sup>3</sup> )	$\omega_b$ (1/s)
Skin	1125	0.42	3600	1620	0.02
Fat	916	0.25	3000	300	$4.58 \times 10^{-4}$ [fx]
Bone	1990	0.37	3100	610	$4.36 \times 10^{-4}$
Brain	1038	0.535	3650	7100	$8.83 \times 10^{-3}$
Sclera	1050	1	3180	0	0
Vitreous	1100	0.60	4178	0	0
Cornea	1050	0.58	4178	0	0

### 2.3. Equations for ELECTROMAGNETIC wave propagation analysis

To simplify the computational analysis, following assumptions have been made for the wave propagation analysis [14].

1. The propagation of the electromagnetic wave is modeled in three dimensions.
2. Electromagnetic wave interacts directly to the human head in the open region.
3. The region outside the head model is truncated by using scattering boundary condition.
4. The dielectric properties of tissues are uniform and constant.

Electromagnetic wave propagation in the human head and free space around it is solved by using Maxwell's equation, as expressed Eq. (1).

$$\nabla \times \frac{1}{\mu_r} \nabla \times \vec{E} - k_0^2 \epsilon_r \vec{E} = 0 \quad (1)$$

$$\epsilon_r = n^2$$

where  $\vec{E}$  is electric field intensity (V/m),  $\mu_r$  is relative magnetic permeability,  $\epsilon_r$  is relative dielectric constant, and  $k_0$  is the free space wave number ( $m^{-1}$ ).

#### 2.3.1. Boundary condition for wave propagation

A half-wave dipole antenna is employed to generate EM waves. The actual part which radiates the EM wave with a specific radiated power is called lumped port (Fig. 1). The boundary condition for the EM wave propagation is shown in Eq. (2).

$$Z_{in} = \frac{V_1}{I_1} = \frac{\vec{E}_1 l_1}{I_1} \quad (2)$$

where  $Z_{in}$  is the input impedance (ohm),  $V_1$  is the voltage along the edges,  $I_1$  is the electric current magnitude (A),  $\vec{E}_1$  is the electric field along the source edge (V/m) and  $l_1$  is the edge length.

The boundary conditions along the interfaces between different mediums, namely, between air and tissues (skin, fat etc.), are considered as a continuity boundary condition:

$$n \times (\vec{E}_1 - \vec{E}_2) = 0 \quad (3)$$

A 3-D perfectly matched layer (PML) has been created outside the model to avoid reflections from emitted electromagnetic wave. Scattering boundary condition is applied on the outer surface of the PML domain, as expressed in Eq. (4)

$$n \times (\nabla \times \vec{E}) - jkn \times (\vec{E} \times n) = -n \times (\vec{E}_0 \times jk(n-k)) \exp(-jk.r) \quad (4)$$

where  $k$  is the wavenumber ( $m^{-1}$ ),  $n$  is the normal vector,  $j = \sqrt{-1}$ , and  $\vec{E}_0$  is the incident plane wave (V/m).

### 2.4. Interaction of electromagnetic waves and human tissues

When the electromagnetic waves propagate through the human head tissues, the energy of electromagnetic waves gets absorbed by the tissues. This absorbed energy is measured in terms of specific absorption rate (SAR). SAR is defined as the power dissipation rate normalized by material density and is described by the following equation [31]:

$$SAR = \frac{\sigma}{\rho} |\vec{E}|^2 \quad (5)$$

where  $\vec{E}$  is electric-field (V/m),  $\sigma$  is electric conductivity (S/m), and  $\rho$  is the tissue density ( $\text{kg}/\text{m}^3$ ).

## 2.5. Equation for heat transfer analysis

For solving the thermal problem, the temperature distribution within the head model is obtained by solving bioheat equation, which takes into consideration heat conduction, blood perfusion, and external heating. The initial temperature is set to  $37^\circ\text{C}$ . Heat transfer analysis is modeled in 3D. To simplify the problem, following assumptions have been made for heat transfer analysis:

1. The human head tissues are biomaterial with uniform and constant thermal properties
2. There is no phase change of substance within the tissues.
3. There is no energy exchange throughout the human head model.
4. There is no chemical reaction within the tissues.

Temperature distribution in the layers of the human head is analyzed by solving Pennes' bioheat equation [14,32,33]. The transient bioheat equation, shown in Eq. (6), efficiently describes how the heat transfer occurs inside the human head.

$$\rho C \frac{\partial T}{\partial t} = \nabla \cdot (k \nabla T) + \rho_b C_b \omega_b (T_b - T) + Q_{met} + Q_{ext} \quad (6)$$

where  $\rho$  is the tissue density ( $\text{kg}/\text{m}^3$ ),  $C$  is the heat capacity of tissue ( $\text{J}/\text{kg}^\circ\text{C}$ ),  $k$  is thermal conductivity of tissue ( $\text{W}/\text{m}^\circ\text{C}$ ),  $T$  is the tissue temperature ( $^\circ\text{C}$ ),  $T_b$  is the temperature of blood ( $^\circ\text{C}$ ),  $\rho_b$  is the density of blood ( $\text{kg}/\text{m}^3$ ),  $C_b$  is the specific heat capacity of blood ( $\text{J}/\text{kg}^\circ\text{C}$ ),  $\omega_b$  is the blood perfusion rate ( $1/\text{s}$ ),  $Q_{met}$  is the metabolism heat source ( $\text{W}/\text{m}^3$ ) and  $Q_{ext}$  is the external heat source term (electromagnetic heat-source density) ( $\text{W}/\text{m}^3$ ).

The heat conduction between tissue and blood flow is approximated by the blood perfusion term,  $\rho_b C_b \omega_b (T_b - T)$ . The external heat source term is equal to the resistive heat generated by electromagnetic field (electromagnetic power absorbed), which is defined as:

$$Q_{ext} = \frac{1}{2} \sigma_{tissue} \left| \vec{E} \right|^2 = \frac{\rho}{2} \cdot SAR \quad (7)$$

Where  $\sigma_{tissue} = 2\pi f \epsilon_r \epsilon_0$

### 2.5.1. Boundary condition for heat transfer analysis

In this simulation heat transfer is considered only in the human head, which does not include parts of the surrounding space. As shown in Fig. 1, the outer surface of the human head corresponding to assumption (3) is considered to be a thermally insulated boundary condition.

$$n.(k \nabla T) = 0 \quad (8)$$

It is assumed that no contact resistance occurs between the tissue layers of the human head. Therefore, the internal boundaries are

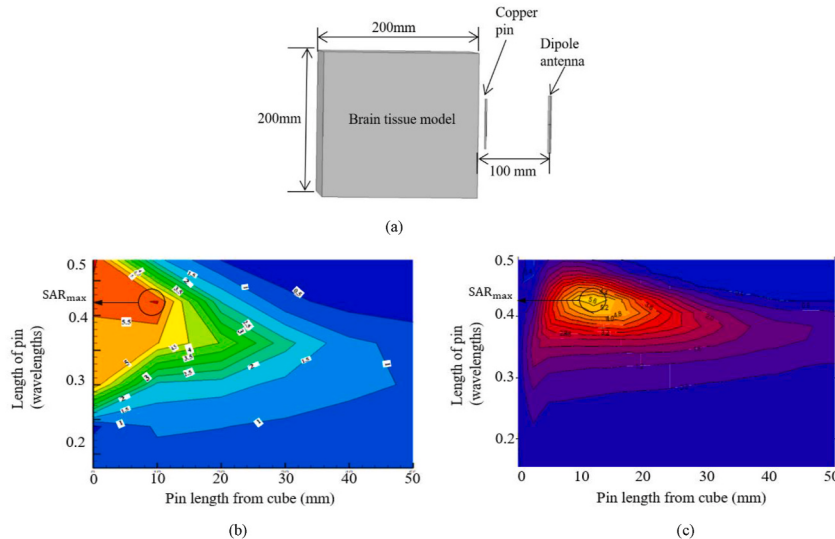


**Fig. 2.** Numerical validation: (a) geometry used for the validation, (b) resultant SAR value from present work, (c) resultant SAR value from Whittow et al. [25].

assumed to be continuous.

$$\nabla T_u = \nabla T_d \quad (9)$$

$$n.(k_u \nabla T_u - k_d \nabla T_d) = 0 \quad (10)$$

### 3. RESULTS and discussion

#### 3.1. Numerical validation

To validate the accuracy of the results obtained from this study. Numerical validation of a previously published work of Whittow et al. [25], has been performed. The model consisting of a cube (brain), copper pin, and a dipole antenna working at 1800 MHz is shown in Fig. 2 (a). The box is irradiated by the dipole antenna from a distance of 100 mm. The pin moves towards the antenna, and for every distance that pin travels its length varies. SAR for each combination of pin's length and position are calculated in the cube. The resultant value of SAR from validation is shown in Fig. 2 (b). The maximum value of SAR obtained in the work of Whittow et al., shown in Fig. 2(c), was found when the pin had 0.42λ length and was at 12 mm distance from the cube. Comparing Fig. 2 (b) from Fig. 2(c), it

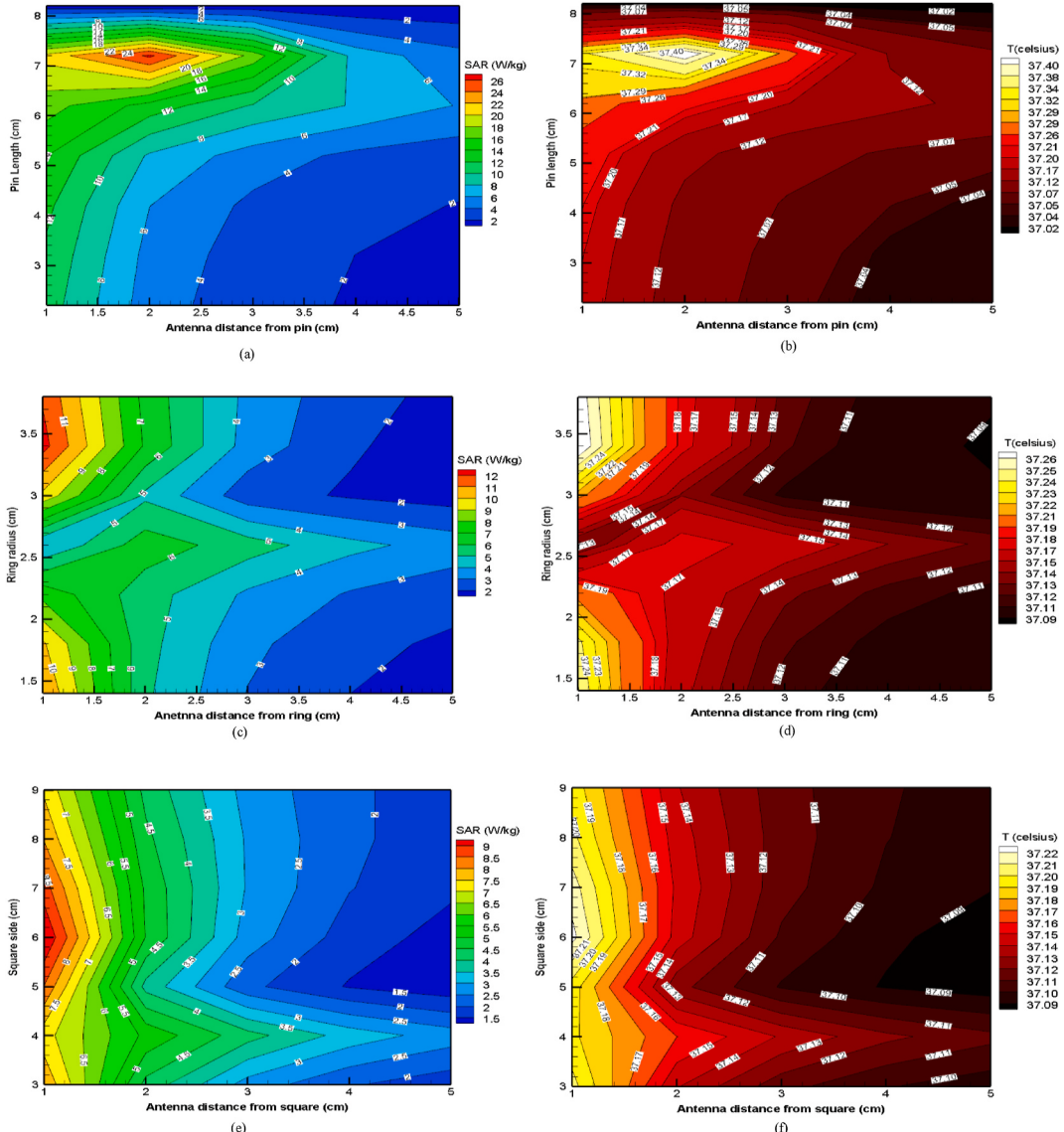


**Fig. 3.** SAR and temperature in the head when dipole antenna move towards the metal objects in voice calling state: pin (a and b), ring (c and d), square (e and f).

can be seen that the obtained SAR results show good agreement with the literature and so builds up confidence in the way of simulating the models for this study.

### 3.2. Effect of metal OBJECT'S size and dipole ANTENNA'S position on SAR and temperature increase in the head model

The size of the metal objects (pin, ring, and square) is varied to investigate its effect on SAR and temperature increase in the head model. The metal objects are placed at a distance of 2 cm from the head model. Dipole antenna is placed at a distance of 5 cm from the metal objects as shown in Fig. 1. Dipole antenna moves towards the metal objects from 5 cm distance to 1 cm distance while metal objects change their size remaining at the same place. This dipole position can be represented as the voice calling position where the ear side of the head gets exposed to the mobile phone. Contour graph of this situation for SAR and temperature increase in the skin layer due to all metal shapes are shown in Fig. 3. The results are obtained for an exposure time period of 30 min from dipole antenna. Electromagnetic radiation generated from the dipole antenna strikes the metal objects and then the head behind the metals. As the metal objects are perfect electric conductor, a secondary current generates on their surfaces. The PEC metals now act like a weak antenna themselves which further irradiates the head. The absorption of electromagnetic energy is then used to calculate the SAR in the head layers as shown in Eq. (5). Dielectric and thermal properties from Tables I and II influence the electromagnetic absorption in the head layers which will later be discussed in detail in section 3.3. The absorbed electromagnetic energy in the layers then gets converted into thermal energy which increases the overall temperature in the head. For pin metal, the highest increase in SAR and temperature are found when pin had the length of 7.2 cm and antenna is 2 cm away from the metal (Fig. 3 (a) and (b)). As the antenna moves further to 1 cm distance, the SAR and temperature decrease in the head layers. This pin length is half of the wavelength of the frequency used, ( $0.42 \times 0.166 \text{ m} = 7.2 \text{ cm}$ ) and only cause the highest value of electromagnetic absorption when antenna is 2 cm away from it. For ring metal, the highest value of SAR and temperature are found when the radius of the ring is 3.4 cm and dipole antenna is 1 cm away from the metal (Fig. 3 (c) and (d)). However, when the ring circumference is of the size of 1 wavelength of the frequency ( $2 \times 3.14 \times 2.6 \text{ cm} = 0.16 \text{ m}$ ), which is 2.6 cm radius of the ring, the power absorption in the head is higher for the 2 cm

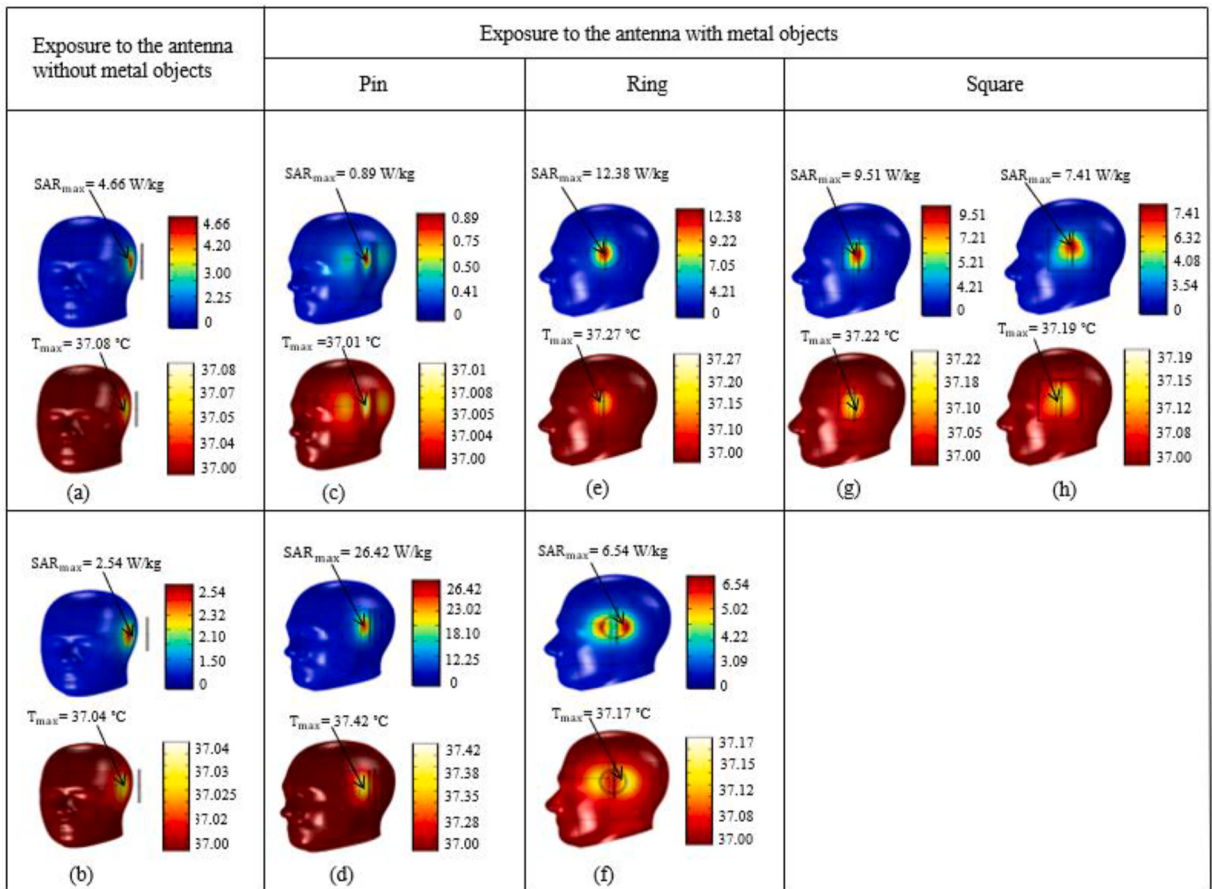


**Fig. 4.** Maximum SAR and Temperature in the head for (a) no metal, antenna 3 cm away from head, (b) no metal, antenna 4 cm away from head, (c) pin length 8.2 cm, antenna 1 cm away from pin, (d) pin length 7.2 cm, antenna 2 cm away from pin, (e) ring radius 3.4 cm, antenna 1 cm away from ring, (f) ring radius 2.6 cm, antenna 2 cm away from ring, (g) square side 6 cm, antenna 1 cm away from square, (h) square side 9 cm, antenna 1 cm away from square.

distance and gets lower for 1 cm distance of antenna from the ring. Similar to the pin in size of half of the wavelength of the frequency used. Lastly, for the square metal, the SAR and temperature were highest when the side of the square is 6 cm (Fig. 3 (e) and (f)), and dipole antenna is 1 cm away from the metal. Unlike pin and ring metal, square metal of all sizes causes the highest EM absorption when dipole antenna is 1 cm away from the metal. Comparing the maximum SAR value caused by pin metal in this study with the SAR value from previous published work of Whittow et al. [25]., In both the cases, pin causes highest value of SAR when was of 7.2 cm length i.e. half of the wavelength of the frequency used.

### 3.3. Maximum value of SAR and temperature caused by the different sizes of metal objects and their effect on the distribution pattern of the absorbed energy on the head model

Fig. 4 (a) and (b) show SAR and temperature distribution, respectively, in the human head when metal objects are absent. In Fig. 4 (a), the antenna is placed at the place where it would have been 1 cm away from the metals (metals being placed at 2 cm away from the head). Now in the absence of the metal object the distance is measured from the head i.e. antenna is 3 cm away from the head model. Likewise, in Fig. 4 (b), the antenna would have been 2 cm away from the metals, now in absence of the metals it is 4 cm away from the head model. When the antenna is 3 cm away from the head model, in absence of metal objects (Fig. 4(a)), the maximum value of SAR and temperature increase in the skin layer are 4.66 W/kg and 37.08 °C , respectively. Whereas, when the antenna is 4 cm away from the head model, in absence of metal objects (Fig. 4(b)), the maximum value of SAR and temperature increase in the skin layer are 2.54 W/kg and 37.04 °C , respectively. Looking at Fig. 4 it is clear that the presence of metal objects influences the SAR and temperature increase as well as the distribution pattern of the absorbed EM energy in the head region. Fig. 4 (d), (e), (f), (g), (h) show increase in the SAR and temperature in the head model when metal objects are present. Fig. 4 (a) is compared with Fig. 4 (e), (g), and (h) when antenna is 3 cm away from the head. Fig. 4 (b) is compared with Fig. 4 (d), (f) when antenna is 4 cm away from the head. This shows presence of metal objects increases the SAR and temperature in the head model. However, presence of metal object also seems to decrease the SAR and temperature in the head. Comparing Fig. 4 (a) with Fig. 4 (c), it can be seen that the pin metal of length 8.2 cm decreases the absorption of energy in the head model. There is also a difference in the energy absorption pattern for different shapes and sizes of the metal objects. Metal objects in Fig. 4 (d), (e), and (g) concentrate the electromagnetic radiation incident on them and then to the head to a smaller area on the head model. This absorption of power increases the SAR and temperature on the head model. Fig. 4 (c) show spreading out of the absorption of energy to a wider area on the head which decreases the SAR and temperature on the head model. Fig. 4 (f) show energy gets absorbed behind the two sides of the ring metal (ring radius 2.6 cm) in which right side of the absorption cause higher value of SAR and temperature. Whereas, Fig. 4 (h) make a triangular shape absorption of power on the head model.

From Fig. 4, the specific sizes of the metal objects that cause highest value of SAR and temperature were known. It is also known that pin and ring metals of resonant sizes show maximum absorption when antenna is 2 cm away whereas for square metal all sizes shows maximum absorption when antenna is closest i.e. at 1 cm away from the metal. The absorption patterns of all three types of metals that caused highest increase in SAR and temperature are shown in Fig. 4 (d), (e) and (g). Tables III and IV show the highest value of SAR and temperature caused by those specific sizes of metal objects in the different layers of the head model. Highest value of SAR is found in the skin layer in presence of pin metal (26.42 W/kg). Whereas, highest value of temperature increase is found in the bone layer in presence of pin metal (37.50 °C). Electromagnetic waves attenuate as they penetrate deeper into the head model. This is why SAR values for the inner layers of the head model are lower. However, the electrical conductivity of brain layer is the highest among all the layers (Table I). The reason even being the furthest tissue in the head model, the SAR value in it is higher than the fat and bone layer of the head model. However, the temperature distribution in the head layers are different. It increases as it penetrates deeper into the head. Skin layer has a higher blood flow ( $\omega_b$ ) that can release heat efficiently while the bone layer has a much lower blood flow that results in poor heat dissipation from the absorbed electromagnetic energy. This shows SAR and temperature do not directly correlate to each other but also depend a lot on the dielectric and thermal properties of the tissues. A bar graph showing EM energy absorption pattern of resonant sizes of the metal objects on skin layer is shown in Fig. 5. The pin and ring objects have higher absorption of EM waves at resonant sizes when the dipole antenna is 2 cm away from the metals. The absorption decreases as the dipole antenna moves closer to the metal objects. This shows a specific distance between metal object and antenna is necessary to cause higher absorption of power. By increasing or decreasing the distance between metal object and antenna causes the mutual coupling between them go out of phase which decreases the power absorption. For square metal, perimeter equals to 1 wavelength of the frequency is chosen ( $4 \times 4 = 0.16$  m). However, power absorption due to all sizes of square metal objects is usual. The power absorption increases as the dipole antenna gets closer to the square metal.

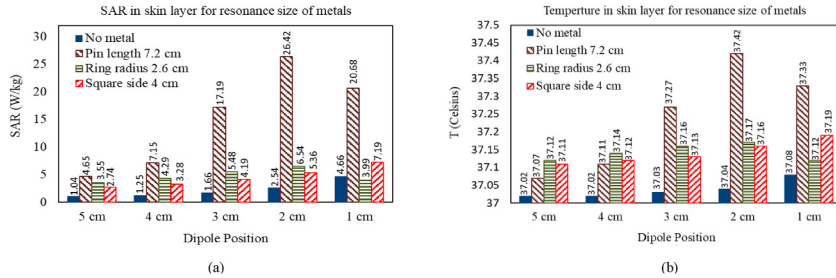
**Table 3**  
Maximum SAR (W/kg) obtained in the head layers for voice calling position.

Head Layers	7.2 cm pin Antenna at 2 cm		3.4 cm radius ring Antenna at 1 cm		6 cm side square Antenna at 1 cm	
	No metal	Pin	No metal	Ring	No metal	Square
skin	2.54	26.42	4.66	12.38	4.66	9.51
Fat	0.44	4.25	0.79	2.13	0.79	1.63
Bone	0.33	3.10	0.60	1.59	0.60	1.14
Brain	2.77	20.68	3.91	10.37	3.91	7.38

**Table 4**

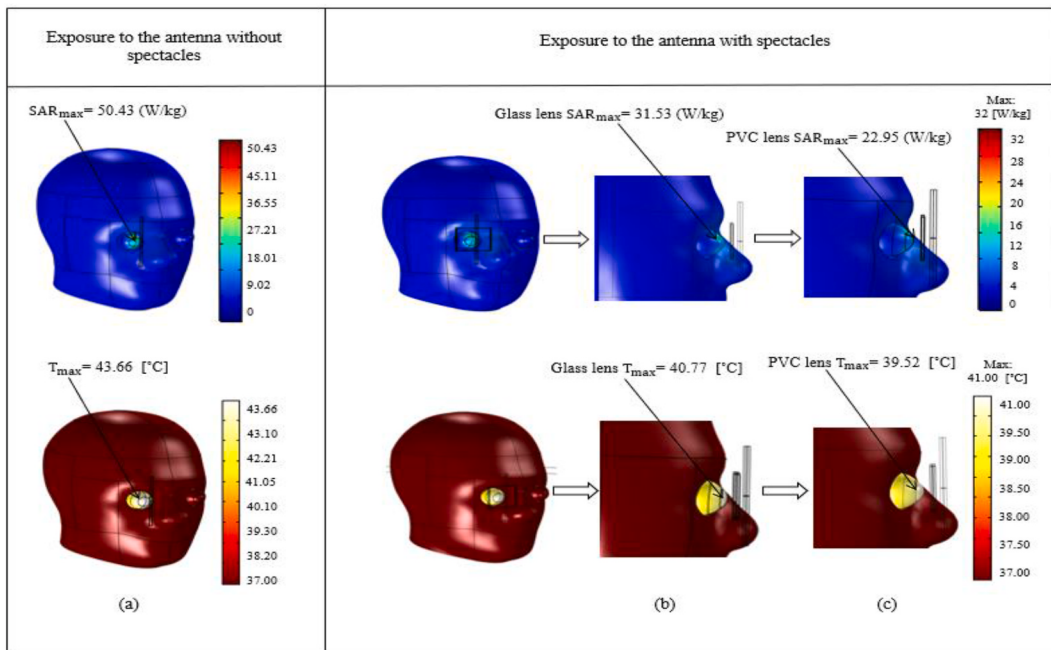
Maximum temperature (°C) obtained in the head layers for voice calling position.

Head Layers	7.2 cm pin Antenna at 2 cm		3.4 cm radius ring Antenna at 1 cm		6 cm side square Antenna at 1 cm	
	No metal	Pin	No metal	Ring	No metal	Square
	skin	37.04	37.42	37.08	37.27	37.08
Fat	37.06	37.49	37.10	37.35	37.10	37.30
Bone	37.06	37.50	37.11	37.41	37.11	37.35
Brain	37.05	37.44	37.09	37.41	37.09	37.35

**Fig. 5.** Comparison of the effect of resonant size of pin (7.2 cm length), ring (2.6 cm radius), and square metal (4 cm side) on (a) SAR and (b) temperature distribution at various dipole position.

### 3.4. Effect of spectacle lenses on SAR and temperature increase in the eye ball layers

Eyes are the most sensitive part of the human body as they have an absence of blood flow which helps to cool down the temperature in the layers. Effect of metal frame spectacles with different types of lenses (PVC and glass) exposed to dipole antenna radiation on eyeball layers is studied. The metal frame (PEC) spectacles are placed 2 cm away from the eyeball. The dipole antenna is placed 5 cm away from the spectacles (Fig. 1). To minimize the computation time, the head model has been simplified by just taking one eye frame of the spectacle. Fig. 6 shows SAR and temperature distribution on the head model in absence and presence of spectacles when head is irradiated from in front (video calling position). It has been found that in presence of spectacle, the SAR and temperature in the eyeball layers decreases. Especially in presence of PVC lens the EM energy absorption is half compared to naked eyes expose to the antenna.

**Fig. 6.** SAR and temperature increase in eyeball at 1800 MHz in the presence of (a) no spectacles, (b) spectacle with glass lens, (c) spectacle with PVC lens.

The SAR and temperature in the eyeball layers were highest when dipole antenna is 1 cm away from the spectacles and 3 cm away from the eyeball in absence of spectacles. However, for the skin around the eyes, the SAR and temperature increase were highest when dipole antenna is 2 cm away from the spectacle. Tables V and VI show the maximum values of SAR and temperature increase, respectively, in the eyeball layers as well as the skin around the eyes. As can be seen from the tables, the spectacle increases the power absorption in the skin layer and decrease it for eyeball layers. The highest SAR is found in the vitreous layer (196.87 W/kg) in the presence of glass lens spectacle. This is because vitreous layer has the highest value of electrical conductivity among all the layers, which makes it absorb more EM radiation (Table I). However, the highest temperature of 43.66 °C is found in the sclera and vitreous layers for without spectacle (Table VI). The temperature increase among the eye ball layers has no major difference, as it has been analyzed without considering the blood perfusion rate (Table II). The temperature generated in the outer layers does not dissipate and transfer the heat to the next adjacent layers. Fig. 7 (a) and (b), respectively, show the comparison of SAR and temperature increase in the skin layer for no spectacles and with spectacles cases. The maximum SAR and temperature increase in skin layer are 29.14 W/kg and 37.12°C, respectively, due to PVC lens. As can be seen from the graphs, for every distance that dipole antenna makes towards the eyes, the SAR increases in the head model. The highest SAR and temperature value in the skin layer occurred when antenna is 2 cm away from the spectacle. This again shows how a specific distance is required between the EM radiating source and the metal to get the highest absorption in the layers. The obtained SAR and temperature values in the eyeball layers exceed the safety limit of 2 W/kg and 1 °C, hence, could lead to some serious damage such as cataract or posterior capsular opacification [9] when exposed to the dipole antenna at the close distance as in this case.

#### 4. Conclusion

This study investigated the SAR and temperature increase inside a heterogeneous human head model when metal objects of various shape and sizes were present in the proximity. The results show different important features to be discussed in the paper. The metal objects definitely alter the absorption of EM radiation in the tissues. In most of the cases, presence of all shapes of metal objects increase the SAR and temperature in the head model for voice calling position. Among all the metal objects, pin metal (7.2 cm length) causes highest increase in energy absorption in the head layers. However, pin metal having a length of 8.2 cm also decreases the energy absorption in the head model compared to when there is no metal object at all. For video calling position, both types of spectacle lenses (glass and PVC) decrease the power absorption in the eye ball layers. There is no major difference in the power absorption for both types of lenses. The skin around the eyes, however, has increased value of SAR and temperature in presence of spectacle lenses. The distance between the dipole antenna and metal objects also affects the energy absorbed in the tissue layers. The power absorption in the tissue layers increases as the dipole antenna moves closer to the metal objects. However, for resonant sizes of pin and ring, the head layers had highest power absorption when dipole antenna is 2 cm away from the metal objects. Skin around the eye area also has higher power absorption when dipole antenna is 2 cm away from the spectacle lenses. It is observed that a specific distance between the antenna and metal objects is necessary to have strong current coupling. Moving the antenna far or closer to that specific position makes the coupling go out of phase which results in low energy absorption in the tissue layers. The size of metal objects affects the distribution of power absorbed in the tissues of the head. In presence of metal objects, the energy gets concentrated to a smaller region on the head which increases the power absorption there, hence, increase in SAR and temperature. The SAR and temperature do not directly correlate with each other and highly depend on the dielectric and thermal properties of tissues. For voice calling position, the maximum value of SAR is found in the skin layer, whereas, bone had the maximum value of temperature increase. For video calling position, SAR is maximum in the vitreous layer of the eyeball, whereas, sclera and vitreous had the maximum value of temperature increase. The maximum SAR and temperature obtained in the voice calling position due to pin metal were 26.42 W/kg and 37.42 °C, respectively, in the skin layer. Here, the SAR exceed the ICNIRP/IEEE (2 W/kg) limit of general public exposure. For video calling position, the maximum SAR and temperature increase were 196.87 W/kg (glass lens in vitreous) and 43.66 °C (no spectacle in sclera and vitreous), respectively. Here, both SAR and temperature obtained were higher than the thresholds for the induction of cataract and opacification formation. This paper, hence, shows how important it is to study temperature distribution along with the SAR distribution to clearly understand the effect of EM radiation on the tissues. Results obtained from this study can help spread awareness among the people who often get exposed to EM radiation wearing some type of metal objects. If the metal objects have size and distance in the range of generating strong coupling interaction with the EM radiation source, this could cause a harmful effect on the health.

#### CRediT authorship contribution statement

**Deepshikha Bhargava:** Conceptualization, Validation, Investigation, Writing - original draft, preparation. **Phadungsak Rattanadecho:** Supervision, Funding acquisition, Project administration. **Teerapot Wessapan:** Visualization, Writing - review & editing.

#### Greek letters

$\mu$	magnetic permeability (H/m)
$\epsilon$	permittivity (F/m)
$\sigma$	electric conductivity (S/m)
$\omega$	angular frequency (rad/s)
$\rho$	density (kg/m³)
$\omega_b$	blood perfusion rate (1/s)

**Table 5**

Maximum SAR (W/Kg) obtained in the head layers for video calling position.

Head Layers	Spectacles Antenna at 1 cm		
	No spec	Glass	PVC
skin	2.51	14.03	21.81
Sclera	50.43	31.53	22.95
Vitreous	195.94	196.87	114.75
Cornea	33.25	24.69	14.50

**Table 6**

Maximum temperature (°C) obtained in the head layers for video calling position.

Head Layers	Spectacles Antenna at 1 cm		
	No spec	Glass	PVC
skin	37.04	37.05	37.08
Sclera	43.66	40.77	39.52
Vitreous	43.66	40.77	39.55
Cornea	43.54	40.68	39.48

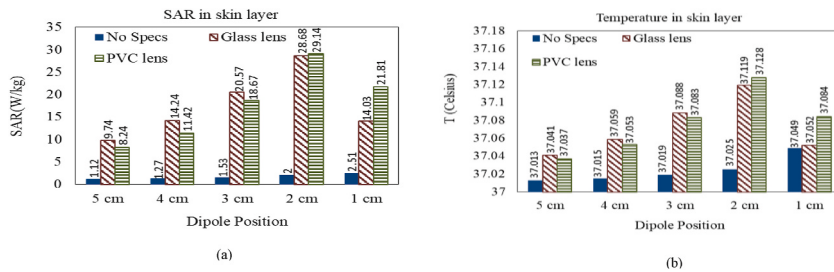


Fig. 7. Comparison of the effect of spectacle lenses on (a) SAR and (b) temperature distribution at various dipole antenna position.

### Subscripts

- b* blood
- ext* external
- met* metabolic
- r* relative
- 0* free space, initial condition

### Declaration of competing interest

The authors declare that they have no known competing financial interests or personal relationships that could have appeared to influence the work reported in this paper.

### Acknowledgments

We would like to acknowledge Thailand Science Research and Innovation and The Thailand Government Budget Grant for Providing Financial support for this study (Grant No. B05F630092).

### References

- [1] O.P. Gandhi, G. Lazzi, C.M. Furse, Electromagnetic absorption in the human head and neck for mobile telephones at 835 and 1900 MHz, *IEEE Trans. Microw. Theor. Tech.* 44 (10) (1996) 1884–1897.
- [2] IEEE Standard for Safety Levels with Respect to Human Exposure to Radio Frequency Electromagnetic Fields, 3 kHz to 300 GHz Amendment 1: Specifies Ceiling Limits for Induced and Contact Current, Clarifies Distinctions between Localized Exposure and Spatial Peak Power Density, 2010, pp. 1–9. IEEE Std C95.1a-2010 (Amendment to IEEE Std C95.1-2005).

- [3] A.B. Ahlbom, J.H. Bernhardt, J.P. Cesarini, L.A. Court, M. Grandolfo, M. Hietanen, A.F. McKinlay, M.H. Repacholi, D.H. Sliney, J.A.J. Stolwijk, M.L. Swicord, L.D. Szabo, M. Taki, T.S. Tenforde, H.P. Jammet, R. Matthes, Guidelines for limiting exposure to time-varying electric, magnetic, and electromagnetic fields (up to 300 GHz), *Health Phys.* 74 (4) (1998) 494–521.
- [4] IEEE-C95.1, IEEE Standard for Safety Levels with Respect to Human Exposure to Radio Frequency Electromagnetic Fields, 3 kHz to 300 GHz,” *IEEE*, NY, USA, 2019, 2019.
- [5] E.R. Adair, B.W. Adams, G.M. Akel, Minimal changes in hypothalamic temperature accompany microwave-induced alteration of thermoregulatory behavior, *Bioelectromagnetics* 5 (1) (1984) 13–30.
- [6] T. Wessapan, S. Srisawatdhisukul, P. Rattanadecho, Specific absorption rate and temperature distributions in human head subjected to mobile phone radiation at different frequencies, *Int. J. Heat Mass Tran.* 55 (1) (2012) 347–359.
- [7] Z.M. Lwin, M. Yokota, Numerical analysis of SAR and temperature distribution in two dimensional human head model based on FDTD parameters and the polarization of electromagnetic wave, *AEU - Int. J. Electr. Commun.* 104 (2019) 91–98.
- [8] P. Bernardi, M. Cavagnaro, S. Pisa, E. Piuzzi, SAR distribution and temperature increase in an anatomical model of the human eye exposed to the field radiated by the user antenna in a wireless LAN, *IEEE Trans. Microw. Theor. Tech.* 46 (12) (1998) 2074–2082.
- [9] T. Wessapan, P. Rattanadecho, Specific absorption rate and temperature increase in human eye subjected to electromagnetic fields at 900 MHz, *J. Heat Tran.* 134 (9) (2012), 091101-11.
- [10] A. Hirata, S. Matsuyama, T. Shiozawa, Temperature rises in the human eye exposed to EM waves in the frequency range 0.6-6 GHz, *IEEE Trans. Electromagn. C.* 42 (4) (2000) 386–393.
- [11] P. Bernardi, M. Cavagnaro, S. Pisa, E. Piuzzi, Specific absorption rate and temperature increases in the head of a cellular-phone user, *IEEE Trans. Microw. Theor. Tech.* 48 (7) (2000) 1118–1126.
- [12] T. Wessapan, P. Rattanadecho, Temperature induced in human organs due to near-field and far-field electromagnetic exposure effects, *Int. J. Heat Mass Tran.* 119 (2018) 65–76.
- [13] P. Keangin, P. Rattanadecho, T. Wessapan, An analysis of heat transfer in liver tissue during microwave ablation using single and double slot antenna, *Int. Commun. Heat Mass Tran.* 38 (6) (2011) 757–766.
- [14] D. Bhargava, N. Leeprechanon, P. Rattanadecho, T. Wessapan, Specific absorption rate and temperature elevation in the human head due to overexposure to mobile phone radiation with different usage patterns, *Int. J. Heat Mass Tran.* 130 (2019) 1178–1188.
- [15] J. Cooper, V. Hombach, Increase in specific absorption rate in human heads arising from implantations, *Electron. Lett.* 32 (24) (1996) 2217–2219.
- [16] R.L. McIntosh, S. Iskra, R.J. McKenzie, J. Chambers, B. Metzenthen, V. Anderson, Assessment of SAR and thermal changes near a cochlear implant system for mobile phone type exposures, *Bioelectromagnetics* 29 (1) (2008) 71–80.
- [17] R.L. McIntosh, V. Anderson, R.J. McKenzie, A numerical evaluation of SAR distribution and temperature changes around a metallic plate in the head of a RF exposed worker, *Bioelectromagnetics* 26 (5) (2005) 377–388.
- [18] M. Olteanu, D. Rafiroiu, “Temperature Increase Due to Specific Absorption Rate Enhancement Around Metallic Stent Implants,” *2011 E-Health And Bioengineering Conference (EHB)*, 2011, pp. 1–3.
- [19] H. Virtanen, J. Huttunen, A. Toropainen, R. Lappalainen, Interaction of mobile phones with superficial passive metallic implants, *Phys. Med. Biol.* 50 (11) (2005) 2689–2700.
- [20] H. Virtanen, J. Keshvari, R. Lappalainen, The effect of authentic metallic implants on the SAR distribution of the head exposed to 900, 1800 and 2450 MHz dipole near field, *Phys. Med. Biol.* 52 (5) (2007) 1221–1236.
- [21] J. Fayos-Fernandez, C. Arranz-Faz, A.M. Martinez-Gonzalez, D. Sanchez-Hernandez, Effect of pierced metallic objects on sar distributions at 900 MHz, *Bioelectromagnetics* 27 (5) (2006) 337–353.
- [22] E. Joó, A. Szász, P. Szendrő, Metal-framed spectacles and implants and specific absorption rate among adults and children using mobile phones at 900/1800/ 2100 MHz, *Electromagn. Biol. Med.* 25 (2) (2006) 103–112.
- [23] W.G. Whittow, R.M. Edwards, A study of changes to specific absorption rates in the human eye close to perfectly conducting spectacles within the radio frequency range 1.5 to 3.0 GHz, *IEEE Trans. Antenn. Propag.* 52 (12) (2004) 3207–3212.
- [24] W.G. Whittow, C.J. Panagamuwa, R.M. Edwards, J.C. Vardaxoglou, The energy absorbed in the human head due to ring-type jewelry and face-illuminating mobile phones using a dipole and a realistic source, *IEEE Trans. Antenn. Propag.* 56 (12) (2008) 3812–3817.
- [25] W.G. Whittow, C.J. Panagamuwa, R.M. Edwards, J.C. Vardaxoglou, On the effects of straight metallic jewellery on the specific absorption rates resulting from face-illuminating radio communication devices at popular cellular frequencies, *Phys. Med. Biol.* 53 (5) (2008) 1167–1182.
- [26] M.H. Mat, M.F. Abd Malek, W.G. Whittow, R. Bibb, Ear prosthesis evaluation: specific absorption rate levels in the head due to different angles and frequencies of electromagnetic exposure, *J. Electromagn. Waves Appl.* 29 (4) (2015) 514–524.
- [27] J.Q. Lan, X. Liang, T. Hong, G.H. Du, On the effects of glasses on the SAR in human head resulting from wireless eyewear devices at phone call state, *Prog. Biophys. Mol. Biol.* 136 (2018) 29–36.
- [28] T. Wessapan, P. Rattanadecho, Numerical analysis of specific absorption rate and heat transfer in human head subjected to mobile phone radiation: effects of user age and radiated power, *J. Heat Tran.* 134 (12) (2012).
- [29] T. Wessapan, P. Rattanadecho, Aqueous humor natural convection of the human eye induced by electromagnetic fields: in the supine position, *J. Med. Bioeng.* 3 (4) (2014) 251–258.
- [30] J. Vencels, M. Birjukovs, J. Kataja, P. Råback, Microwave heating of water in a rectangular waveguide: validating EOF-Library against COMSOL multiphysics and existing numerical studies, *Case Studies Thermal Eng.* 15 (2019) 100530.
- [31] V. Stanković, D. Jovanović, D. Krstić, V. Marković, N. Cvetković, “Temperature distribution and Specific Absorption Rate inside a child’s head, *Int. J. Heat Mass Tran.* 104 (2017) 559–565.
- [32] B. Kundu, D. Dewanjee, A new method for non-Fourier thermal response in a single layer skin tissue, *Case Studies Thermal Eng.* 5 (2015) 79–88.
- [33] T. Wessapan, S. Srisawatdhisukul, P. Rattanadecho, Numerical analysis of specific absorption rate and heat transfer in the human body exposed to leakage electromagnetic field at 915 MHz and 2450 MHz, *J. Heat Tran.* 133 (5) (2011).